Block Copolymer Containing PEG and Histamine-like Segments: Well-Defined Function for Gene Delivery

Journal:	*New Journal of Chemistry*
Manuscript ID	NJ-ART-12-2015-003641.R1
Article Type:	Paper
Date Submitted by the Author:	02-Jun-2016
Complete List of Authors:	Li, Junbo; College of Chemical Engineering & Pharmaceutics, Henan University of Science & Technology Zhao, Jianlong; Henan University of Science & Technology Gao, Jiayu; Henan University of Science & Technology, School of Chemical Engineering & Pharmaceutics Liang, Ju; College of Chemical Engineering & Pharmaceutics,, Henan University of Science & Technology Wu, Wenlan; College of Chemical Engineering & Pharmaceutics,, Henan University of Science & Technology Liang, Lijuan; Henan University of Science & Technology, School of Chemical Engineering & Pharmaceutics

Block Copolymer Containing PEG and Histamine-like Segments: Well-Defined Function for Gene Delivery

Junbo Li[1]*, Jianlong Zhao[2], Jiayu Gao[1], Ju Liang[1], Wenlan Wu[2], Lijuan Liang[1]

[1]School of Chemical Engineering & Pharmaceutics, Henan University of Science & Technology, Luo Yang 471023, China; [2]School of Medicine, Henan University of Science & Technology, Luo Yang 471023, China

Abstract

The delivery of genetic material to cells provides a promising treatment approach to many genetic diseases. Rational structure design for reducing the toxicity while improving transfection efficiency is an important strategy for development of safe and highly efficient polycation gene vectors. In this study, a novel block copolymer composing of PEG and cationic histamine-like segments, was synthesized by reversible addition-fragmentation chain transfer (RAFT) polymerization and subsequently explored its potential of gene vector *in vitro*. The block copolymer showed a lower cytotoxicity to three cell lines. After complexing with pEGFP-C1, the resulting DNA-encapsulated micelles possessed uniform small size, high salt and serum tolerance which were confirmed by dynamic light scatter (DLS) and transmission electron microscopy (TEM). Highly efficient gene transfection was further obtained in human liver carcinoma (HepG2) *in vitro*. The low cytotoxicity and high transfection stem from the well-defined functions of different moiety, PEG segment, imidazolium and amine group on histamine-like pendant contributing to the different steps of gene delivery, including colloid stability, highly effective DNA condensation and endosomal escape respectively.

Key Words: Block copolymer; RAFT polymerization; Micelles, Gene vector, Transfection efficiency.

---

*Corresponding author. Tel: +86 379 64231914; Fax: +86 379 64232193

E-mail address: Lijunbo@haust.edu.cn (J.B. Li).

Introduction

Using foreign nucleic acid to repair defective genes, gene therapy has provided a promising treatment strategy for some severe diseases caused by genetic defects, such as Parkinson's disease[1-3] and cancer[4, 5]. Introducing genetic material into target cells, gene therapy requires efficient and safe gene delivery systems without causing any associated pathogenic effects[6, 7]. Therefore, the synthetic gene vectors[8, 9] are highly desirable for the development of gene delivery systems due to their low immunogenic response, easy structure modification, capability to carry large inserts when compared to viral vectors.

Synthetic gene vectors, especially polymers, have manifested great potential in human gene therapy due to their tailored size, structure, and functionality for specific therapeutic needs[4, 10]. Until now, several cationic polyamine[11, 12], such as poly-L-lysine (PLL), polyethyleneimine (PEI), and chitosan have demonstrated the ability to condense and deliver plasmid DNA to different cell lines[13]. The resulting nanoparticles or polyplexes can effectively protect the nucleic acids from enzymatic degradation and facilitates cellular uptake because of their cationic surface. However, it will be inevitable to bring the cytotoxicity and undesired aggregation *in vivo*[14, 15]. Moreover, the random interaction also causes a large size and polydisperse polyplexes, leading to low transfection efficiency[16, 17]. Therefore, how to reduce the toxicity while improve transfection efficiency is still an important issue for cationic polymers as gene carriers in clinical application[18].

To address this issue, many efforts have been made to increase availability through optimizing polymeric structure. An effective approach to reduce acute toxicity is modification of cationic polymers with PEG. PEG has hydrophilic, non-ionic nature and is one of the most widely used biocompatible polymers in drug delivery[19, 20]. The PEG grafted or copolymerized polymers complex with anionic DNA produced a core-shell polymeric micelles, where the polycation-DNA complex made up the core and the hydrophilic PEG segment made up the shell. The hydrophilic PEG-shell has been confirmed can increase colloid solubility, reduce systematic toxicity and

improve circulation time[19, 21, 22]. For instance, compared to PLL/DNA complexes, polyion complex micelles from complexes of PEG-*b*-PLL with DNA has exhibited a high stability in a serum containing medium and prolonged blood circulation in experimental animals[23]. Moreover, the Kataoka's group firstly compared the different dynamic states of polyplexes and PEGylated polyplex micelles in the bloodstream, and demonstrated the significance of PEGylation to prevent polyplexes agglomeration *in vivo*[24]. However, further enhancing transfection ability is indispensible for the development of PEGylated polyplex micelles because the shell was supposed to impair their cellular uptake[25].

The other approach is polymers modified with biomolecules[26, 27]. As a moiety of histamine, imidazole ring has been employed to modify polymeric vectors for enhancing biocompatibility and gene transfection efficiency due to its buffering capacity near endosomal pH, which promote a fast endosomal escape via so-called "proton sponge" effect[26-29]. Moreover, considering the deprotonation as the physiological pH, the imidazole moiety was further quaternized for improvement of DNA-binding ability[30, 31]. The resulting imidazolium polymers have a permanent positive charge and a low cytotoxicity on account of reducing the cationic charge density through spread electrons around the N-heterocycle[32]. For example, Long *et al*. prepared the imidazolium-based copolymers via functionalized 1-vinylimidazole homopolymers with hydroxyl functionalized alkyl chains, and then investigated the relationship between the degree of quaternization and DNA binding, cytotoxicity, and *in vitro* transfection efficiency[33]. It was found that DNA binding increased with the increase in degree of quaternization, but a negative tendency on transfection efficiency. The discrepancy probably comes from the competition between the buffering capacity and the DNA binding affinity from imidazole and imidazolium moiety. Therefore, the polycation vector with well-defined function is necessary to development of safe and efficient polycationic gene delivery system.

Here, a novel block copolymer, polyethylene glycol-*b*-poly1-(3-aminopropyl)-3-(2-methacryloyloxy propylimidazolium bromine) (PEG-*b*-PAMPImB) was prepared by reversible addition-fragmentation chain transfer

(RAFT) polymerization to construct DNA-encapsulated micelle for gene delivery. The PEG shell was designed to protect colloid stability from aggregation in physiological condition. The permanent positive charge imidazolium was used for high efficient DNA condensation. The amine was expected to provide buffering capacity in endosome for fast endosomal escape. The process of forming polyplex micelles and DNA delivery is illustrated in Scheme 1.

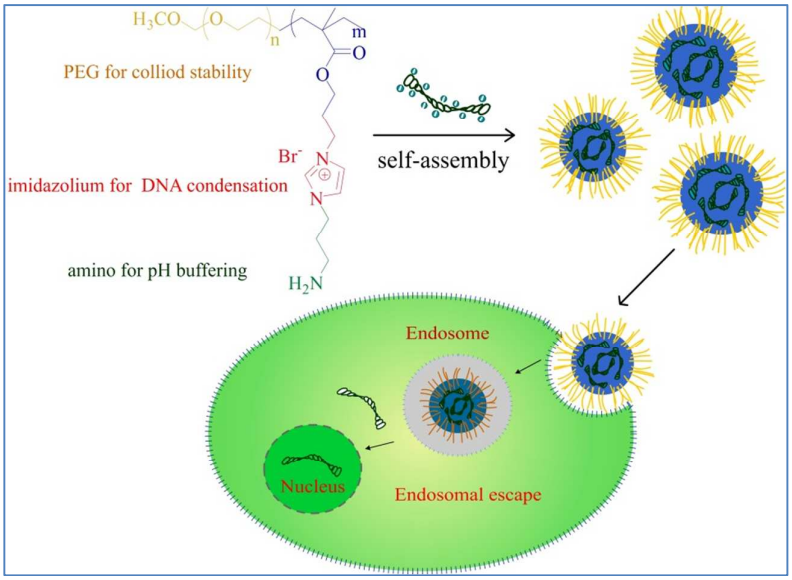

Scheme 1. Schematic representation of forming polyplex micelles and DNA delivery.

2. Experimental section

2.1 Materials

Polyethylene glycol monomethyl ether (CH_3O-PEG_{112}-OH) (Mw=5000 and the polydispersity index PDI=1.05) was purchased from Sigma and used as received. 2, 2'-Azobis(isobutyronitrile) (AIBN) (97%) was purchased from J&K Chemical and recrystallized before use as an initiator. The monomers, 1-(3-aminopropyl)-3-(2-methacryloyloxy propylimidazolium bromine) (AMPImB), and macro-RAFT agent, PEG-CTA were synthesized according to the literature procedure [34-36] (the detailed synthesis is shown in support information). Dulbecco's modified Eagle's medium (DMEM), penicillin-streptomycin, trypsin-EDTA, fetal bovine serum (FBS), 3-[4,5-dimethylthiazol-2-yl]-2,5-diphenyltetrazolium bromide (MTT), and Dubelcco's

phosphate buffered saline (DPBS) were purchased from Invitrogen Corp. The reporter plasmid, enhanced green fluorescent protein gene (pEGFP-Cl), was purchased from Invitrogen and Promega, amplified in *Escherichia coli* and purified by E.Z.N.A. fast filter endo-free plasmid maxi kit (Omega). The pEGFP-C1 was stored at -20^{o}C before the transfection experiments. Branched poly(ethylenimine) (bPEI-25k) was obtained from Aldrich-Sigma Chemical. All other reagents were analytical grade and used as received.

2.2 Synthesis of block copolymer PEG-b-PAMPImB

PEG_{112}-CTA (0.31g, 0.06 mmol), AIBN (2.0 mg, 0.0012mmol), AMPImaB (1.23g, 0.03mol), and dry DMF (1.0mL) were placed in a sealed dry ampule. After the solution was degassed using three freeze-pump-thaw cycles, the polymerization was conducted at 60 ^{o}C over 24h. The reaction mixture was purified using a two-step precipitation in ethyl acetate and isolated by filtration, obtaining PEG-*b*-PAMPImB as a light pink powder. Dithioester-terminated PEG-*b*-PAMPImB was finally reduced by hydrazine for decrease cytotoxicity. To a 100 mL round-bottom flask equipped with a magnetic stirring bar, 0.3 g of dithioester-terminated PEG-*b*-PAMPImB was dissolved in 30 mL of dry alcohol; 1 ml of 1.0 M aqueous hydrazine solution was added under vigorous stirring. The reaction mixture was stirred at room temperature for more than 3 days and eventually precipitated in THF. The final composite and structure of PEG-*b*-PAMPImB was determined by ^{1}HNMR and gel permeation chromatography (GPC). ^{1}HNMR spectroscopy was recorded on a Bruker AV300 spectrometer. The molecular weight distribution (M_w/M_n) of the polymer was characterized by using a Waters 600E gel permeation chromatography (GPC) analysis system equipped with Waters Styragel HT column with Poly(ethylene oxide) as the calibration standard and water (with 8.5 g/L $NaNO_3$) as the eluent (flow rate: 0.4 mL/min). The synthesis procedures are illustrated in Scheme 2:

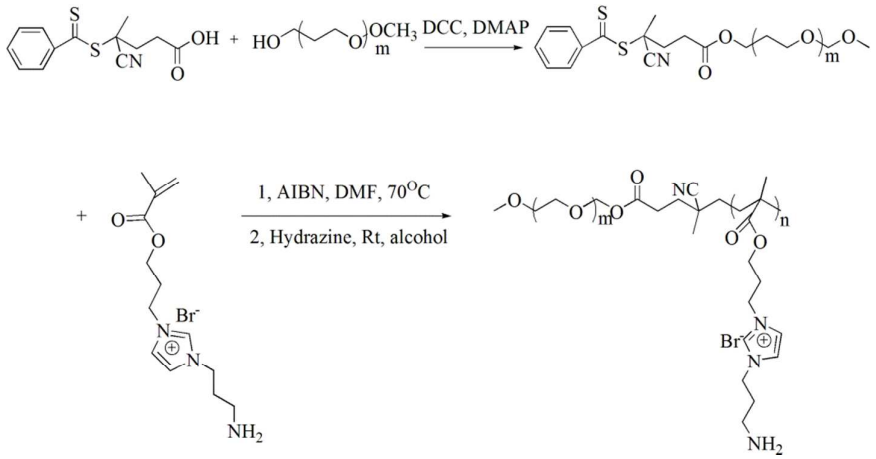

Scheme 2. Synthetic scheme for PEG-CTA and PEG-*b*-PAMPImB.

2.3 Cell Culture:

HepG2, HeLa and 293T cells were cultured in the DMEM medium supplemented with 10% (v/v) heat-inactivated FBS and 1% penicillin-streptomycin at room temperature in a humidified atmosphere containing 5% CO_2.

2.4 Preparation of polyplex micelles:

Polyplex micelles at various charge ratios were prepared by dropping polymer of 0.2mg/mL into an equal volume of plasmid DNA. The concentration of plasmid DNA solution was 200ng/μl in aqueous solution. The gentle vortexing and 30 min incubation at room temperature ensured the stable formation of micelles.

2.5 Agarose gel electrophoresis：

The PEG-*b*-PAMPImB/DNA complexes with different charge ratio ranging from 0/1 to 10/1 were prepared according to the conditions described above. The binding efficiency was studied through gel retardation assay. After 30 min incubation at room temperature, complex solutions were analyzed by 1% agarose gel electrophoresis (100 V, 30 min). DNA retardation was visualized by irradiation with UV light and assayed with Cam2com software.

2.6 Measurement of micellar size and zeta-potential:

The PEG-*b*-PAMPImB/DNA complexes with different charge ratios were prepared

according to above procedure. The stocking solution of complexes was diluted by distilled water to 1mL for zeta-potential measurement. The micellar solution of different medium was prepared by diluting stocking solution in HEPES, 150mM NaCl and 10% FBS solution for particle size measurement. After incubating for 30 min at room temperature, the average particle size and zeta-potential of the complexes were determined by using a Zeta Potential/BI-90Plus Particle Size Analyzer (Brookhaven, USA). Transmission electron microscopy (TEM) measurements were conducted using a JEM-2100 electron microscope at an acceleration voltage of 200kV; a small drop of micellar solution was deposited onto a carbon-coated copper EM grid and dried at room temperature under atmospheric pressure.

2.9 Cytotoxicity assay:

HepG2, HeLa and 293T cells were seeded into 96-well plates at 5000 cells/well and cultured 24h in 200μl DMEM containing 10% FBS. PEG-*b*-PAMPImB and PEI25k with different concentrations were prepared in the PBS (pH 7.4) solution. The PEG-*b*-PAMPImB or the PEI solution of 20μl was added to each well, followed by incubation of the cells for 24 h. After that, the medium was replaced with 200μl of fresh medium. MTT (20μl, 5mg/ml in PBS) stock solution was then added to each well. After 4 h, unreacted dye was carefully removed, and the formazan crystals were dissolved by 200μl/well DMSO. The plate was incubated for another 10 min before using absorbance at 570 nm to measure by an ELISA microplate reader (Bio-Rad). The cell viability (%) was calculated as: cell viability (%) = $(OD_{sample}/OD_{control})\cdot 100$, where OD_{sample} is the absorbance of the cells treated by polymers, and $OD_{control}$ is the absorbance of the untreated cells. Each experiment was done in triplicate.

2.10 In vitro transfection:

To study the transfection activity of the micelles, HepG2 cells were seeded into 24-well plates at an initial density of $5\cdot 10^4$ cells/well with 1 mL DMEM containing 10% FBS and incubated at 37°C for 24 h in 5% CO_2 (to reach 70% confluence at the time of transfection). The cells were incubated with the micelles, Lipofectamine2000/DNA

and PEI/DNA at 10/1 complexes with in serum-free culture medium for 4 h at 37°C. At the time of transfection, the medium was replaced with fresh medium containing 10% serum and incubated for 48h at 37°C. The cells were monitored for green fluorescence protein (GFP) expression with a fluorescence microscope. The cells were washed with PBS three times, fixed with 4% paraformaldehyde for 30 min and then observed with a confocal laser scanning microscope (LSM 780，Zeiss).

2.11 Transfection efficiency assay:

Transfection efficiency assay was determined by flow cytometry to quantify the percentage of GFP expressing cells. HepG2 cells (10^5 cells/well) were seeded in 6-well plates in 2ml of the growth medium (DMEM with 10% FBS) for 24 h. The original medium was replaced with 2.0 ml of the fresh growth medium containing polyplex/DNA complexes with different charge ratio. After incubated for 4 h at 37°C, the harvested cells were washed with PBS, detached with 0.25% trypsin and then resuspended with 500μl PBS (pH 7.4). Finally, transfection efficiency was carried out using a flow cytometer (FC500, Beckman Coulter).

3. Results and discussion

3.1. Polymer synthesis and characterization

The RAFT approach was commonly applied to the polymerization of ionic monomers and obtained relative homopolymers[34, 35] and copolymers[36] with controlled molecular weights and narrow polydispersity. Here, 1-(3-aminopropyl)-3-(2-methacryloyloxy propylimidazolium bromine) was first prepared, and then employed to chain-extend PEG-CTA by RAFT polymerization. The structure and composite of resulting PEG-*b*-PAMPImB was determined by ^{1}HNMR and GPC. The ^{1}HNMR spectrum of PEG-*b*-PAMPImB in D_2O is shown in Fig. 1A. From Fig. 1A, the characteristic H of AMPImB (saw in support information) is showed clearly at the peak of a, b, c, d and e. Besides PAMPImB segment, the characteristic at f is attributed to PEG. The ratio of the area of peak a to f was 1: 4.3, which can be used to calculate the composition of PEG-*b*-PAMPImB. Therefore, the

block copolymer can be denoted as PEG_{112}-*b*-$PAMPImB_{96}$ with the subscript indicating the number of the repeating units. Thus, the molecular weight of PMMPImB is 34790 calculated by NMR. The polydispersity indexes of PEG_{112}-CTA and PEG_{112}-b-$PAMPImB_{96}$ measured by GPC (Fig.1B) are 1.05 and 1.15 respectively.

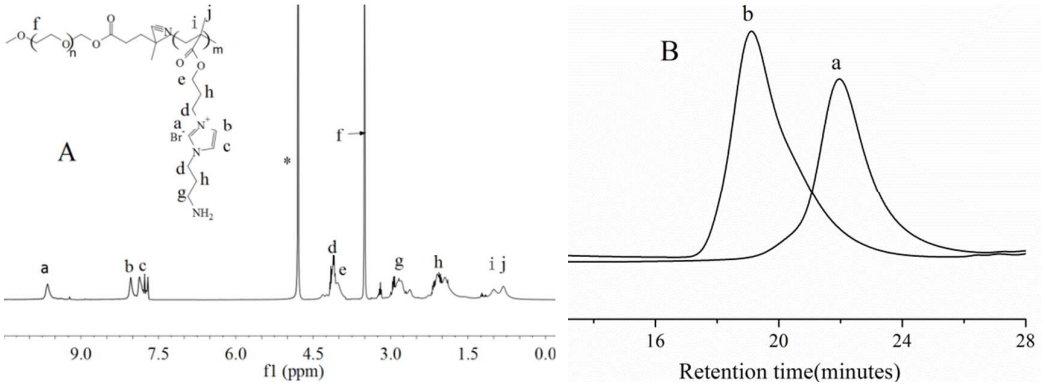

Fig. 1. ^{1}H NMR spectra of PEG_{113}-*b*-$PMMPImB_{96}$ in D_2O at room temperature (A); GPC traces for PEG-CTA (a) in water and PEG_{113}-*b*-$PMMPImB_{96}$ (b) in 8.5g/L $NaNO_3$ water solution at room temperature (B).

3.2 Cell viability

Low cytotoxicity is a highly desired property of a polycation for application in drug and gene delivery[37]. Fig.2 shows the results of *in vitro* cytotoxicity studies of PEG-*b*-PAMPImB in HepG2, HeLa and 293T cells and PEI25kD in HepG2 by MTT assay at various concentrations. The sample without treatment of PEG-*b*-PAMPImB and PEI25k was considered as a control with a cell viability of 100%. From Fig.2, the PEG-*b*-PAMPImB exhibits much lower cytotoxicity against the three type cell lines compared with PEI25kD against HepG2. The viability of cells is kept above 85% even at the concentration 200μg/L. The PEI has high positive charge density, which can interact with cell membranes and inhibit normal cellular processes, resulting to high cytotoxicity. PEG-*b*-PAMPImB is composed of non-ionic and biocompatible PEG and cationic histamine-like segment. PEGlation can help to improve the biocompatibility of unmodified analog. Besides, imidazolium cation has a resonance-stabilized electrons structure, where the positive charge can spread around the N-heterocycle for reducing positive charge density.

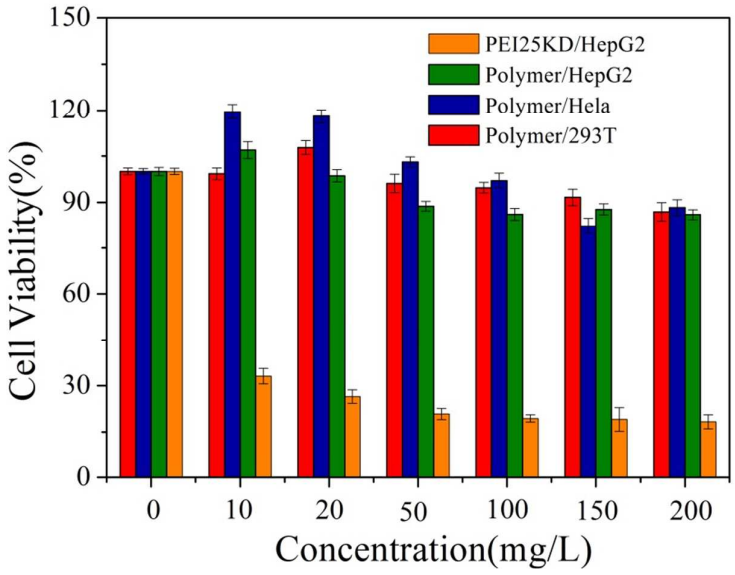

Fig.2. Cytotoxicity of PEG-*b*-PAMPImB against HepG2 (PEI25 kDa as a control), HeLa and 293T cells at various concentrations. Values represent mean (SD (n = 3)).

3.3 Aagrose gel electrophoresis and zeta-potential

Gel electrophoresis assays can determine the effective amount of polymer to bind DNA for delivery. The migration of naked DNA and PEG-*b*-PAMPImB/DNA complexes at charge ratios ranging from 0/1 to 10/1 is shown in Fig.3A. From Fig.3A, the migration of DNA in agarose gel has completely been retarded when the charge ratio was above 3. The result indicates that PEG-*b*-PAMPImB possesses a good DNA binding ability. Commonly, the optimum charge ratio in electrophoresis only represents the critical ratio for retardation. However, the ratio for transfection is usually higher than that for gel retardation assay, as demonstrated in many published works. The zeta-potentials upon charge ratios were shown in Fig. 3B. Fig. 3B exhibits an increase trend along with the increase of charge ratios. At high ratios, the zeta-potentials are observed to reach a maximum plateau. The negative charge of the DNA is rapidly neutralized by the excess positive charge of PAMPImB. The surface charge of the polyplex presents positive value when the ratios above 4, which facilitate cellular internalization through interaction with negatively charged cell membrane.

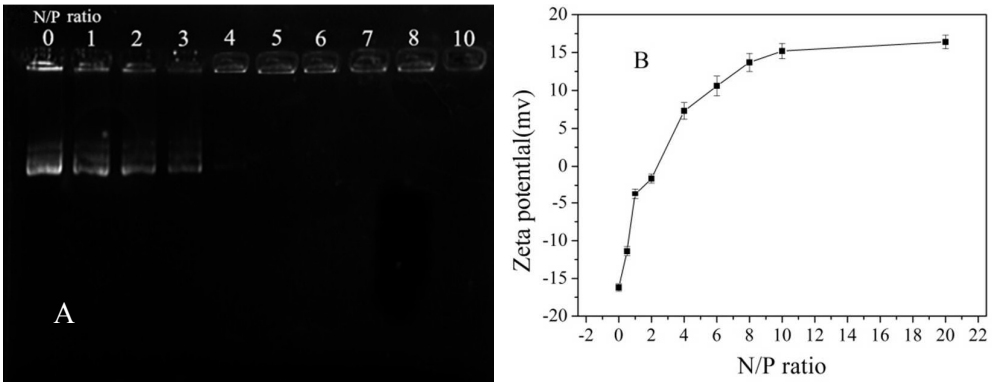

Fig.3. Gel retardation assay (A) and zeta-potentials (B) for naked plasmid DNA and PEG-*b*-PAMPImB/DNA complexes in pure water at various N/P ratios. Values represent mean (SD (n = 3))

3.4 Morphology and colloidal stability of micelles

It is an essential process that mediates the endocytosis of complexes via efficient compaction of DNA into nanoparticles by polycation. Commonly, cell is able to take up particles ranging from tens to hundreds nanometer. However, the nanoparticles with uniform and small (under 200nm) size are desired because of their enhanced bioavailability and ability to take advantage of the enhanced permeation and retention (EPR) effect[38]. Meanwhile, the stability of polyplexes under physiological conditions is an important influence on gene expression *in vitro* and further application *in vivo*[39]. Here, the solutions of PEG-*b*-PAMPImB and pEGFP-C1 were firstly mixed in pure water under the different charge ratio, and then transferred into HEPES buffer (20 mM, pH 7.4), 150mM NaCl and 10% FBS solution, respectively. After 4 hours incubating, the average hydrodynamic diameter (D_h) and polydispersity index (PDI) were measured by DLS and listed in Tab.1. As revealed in Tab.1, PEG-*b*-PAMPImB efficiently condenses DNA into nanoscale particles in pure water. The D_h increase from 95 to 138 nm and the PDI broadens with increase of the ratio from 4/1 to 20/1. In each sample, the weight of DNA was fixed at 200ng. The high charge ratio means that the excess polymers are used to condense DNA, giving rise to polydisperse structure due to electrostatic repulsion between unneutralized positive groups. The micelles can be stably existed in the HEPES buffer (pH7.4) and 150mM NaCl solution, as demonstrated by a slight change of its D_h and PDI under four ratios.

However, all the D_h of micelles in 10% FBS shows a slight increase, and the PDI broadens when the ratio above 6/1. The increased D_h and broadened PDI can be attributed to protein adsorption via electrostatic attraction in FBS. At the same time, the additional components make PDI broaden.

Tab.1. the hydrodynamic diameter and polydispersity index of polyplex micelles at different ratio and medium.

N/P	Pure water		HEPES (pH 7.4)		150mM NaCl		10%FBS	
	D_h(nm)	PDI	D_h(nm)	PDI	D_h(nm)	PDI	D_h(nm)	PDI
20/1	138	0.19	140	0.20	136	0.18	153	0.27
10/1	126	0.18	121	0.19	123	0.19	133	0.24
6/1	101	0.11	97	0.13	105	0.10	122	0.15
4/1	95	0.08	94	0.07	97	0.09	106	0.10

Fig.4 showed the TEM image of micelles at three ratios (10/1, 6/1 and 4/1) in pure water. From Fig. 4a, a clear loose and polydisperse structure is found in the micelles at 10/1. After decreasing the N/P to 6/1 (Fig. 4b) and 4/1 (Fig. 4c), the images show the morphology of spherical micelles turns to dense and the size becomes uniform gradually, consistent with the results of DLS. As above discussion, the high charge ratio means high positive zeta-potential in system, leading to a lot of cationic groups no access to DNA making a loose structure due to electrostatic repulsion between the unbound polyionic blocks in micellar core. With the decrease of zeta-potential, the size of micelles turns to be shrinking and uniform. Moreover, all micelles disperse well even if at high charge ratio, owning to the steric protection from outer shell of PEG.

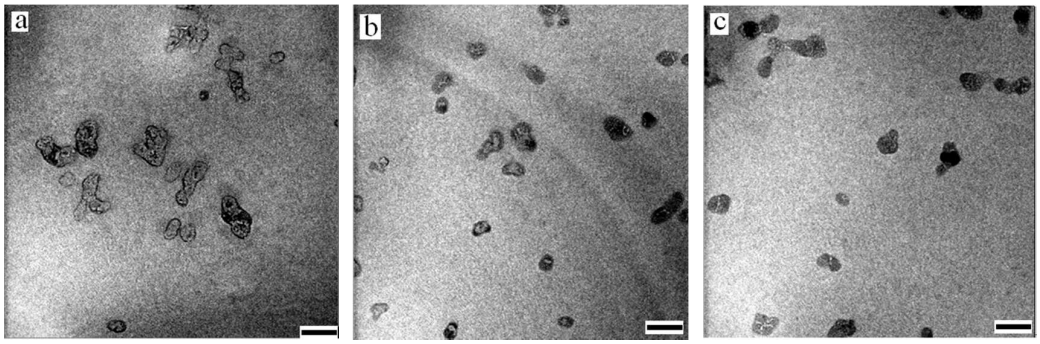

Fig. 4. TEM images of the micelles forming at the charge ratio of 10/1 (a), 6/1 (b) and 4/1 (c) in the presence of pure water. The scale bar is 100nm.

The morphology of the PEG-*b*-PAMPImB/pEGFP-C1 micelles (N/P ratio at 4/1) in different media was observed by TEM and shown in Fig.5. From Fig.5a, the micelles in pure water show spherical nanoparticles with a diameter of 80-95 nm, implying that DNA was tightly packed into the micellar core. After removed to HEPES buffer and 150mM NaCl solution, the micelles remain the uniform sphere and no aggregation. Change of size is observed in Fig. 5b and 5c. Fig.5d is the TEM of micelles in 10% FBS, keeping well dispersion and individual sphere. The size shows a slight increase similar to the result in DLS. Supporting by the results of DLS and TEM, it confirms that PEG-*b*-PAMPImB has high ability to condense DNA and form the polyplex micelles with uniform size, high stability and good salt and serum tolerance. The permanent positive imidazolium can compact negative DNA free from the changes of external conditions, such as pH value and salt concentration. The shell of PEG provides static shielding and colloidal stability.

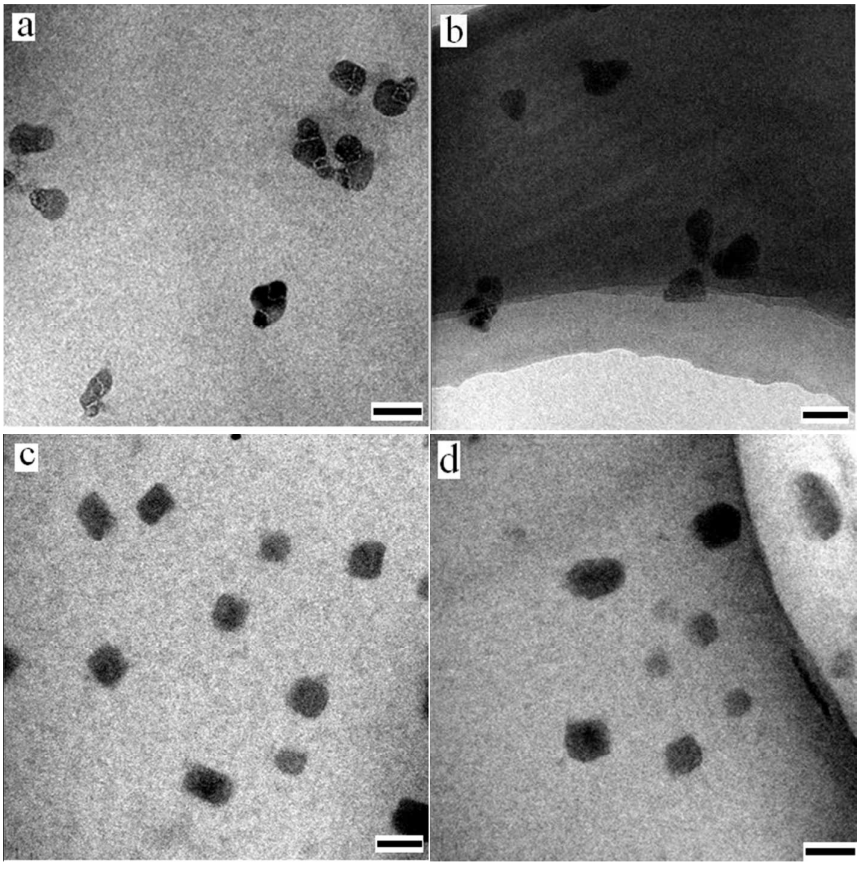

Fig. 5. TEM images of the micelles forming at the charge ratio of 4/1 in the presenceof pure water(a), HEPES buffer(b), 150mM NaCl(c) and 10% FBS(d). The scale bar is 100nm.

3.5 In vitro gene transfection

The pEGFP-C1 was employed as a reporter gene for evaluating transfection efficiency of polyplex micelles to HepG2 cells *in vitro*. Vectors were selected the micelles at four charge ratios (4/1, 6/1, 10/1 and 20/1). Besides, the naked DNA, and commercial transfection reagents Lipofectamine2000 and PEI25K (N/P of 4/1), was used as negative and positive controls, respectively. The transfection efficiency was quantified by flow cytometry in accordance with the cell population of green fluorescent proteins (GFP) expression. Fig.6A shows the percentage of the cells expressing GFP mediated by above vectors. Interestingly, micellar vector forming at charge ratio of 4/1 shows the optimal transfection efficiency of about 71%, which is superior to Lipofectamine2000, PEI/DNA and other ratio micelles. The transfection efficiency presents the decrease tendency along with the increase of charge ratio, indicating that has a relation with the size and dispersion degree of vector. According to the result of DLS and TEM, the polyplex micelles of 4/1 possesses smaller uniform size and higher collide stability, which always help to the cellar internalization and improve the transfection efficiency[40, 41]. The transfected cells were directly observed by a reverse fluorescent microscope and the result was presented in Fig.6B. After a 24 hours post-transfection period, micelles vector at charge ratio of 4/1 also displayed the highest transfection activity among the vectors. The GFPs are distributed within the whole cytosol and nucleus from the image of confocal laser scanning microscopy (Fig.6C), further determining that a high expression of GFP to HepG2 cell mediating by polyplexes micelles at ratio of 4/1.

Actually, successful gene expression requires gene vectors with the capacity of across the cellar membrane, endosomal escape, and final delivery of genetic cargo into the cytosol or nucleus. Commonly, endosomal escape of polyplexes can achieve by means of polymer protonation in the endosome, inducing endosomal rupture and

facilitating gene delivery. Here, the high transfection efficiency of polymeric micelles is attributed to low cytotoxicity, uniform size and stronger buffering capacity of amino group, which were demonstrated by the contrast test via an analog polymer without amino group. Poly(ethylene glycol)-block-poly[1-methyl- 3-(2-methacryloyloxy propylimidazolium bromine), reported in our previous paper[36], also has the ability to condense DNA to polyplex micelles (date not shown), but cannot observed significant GFP expression.

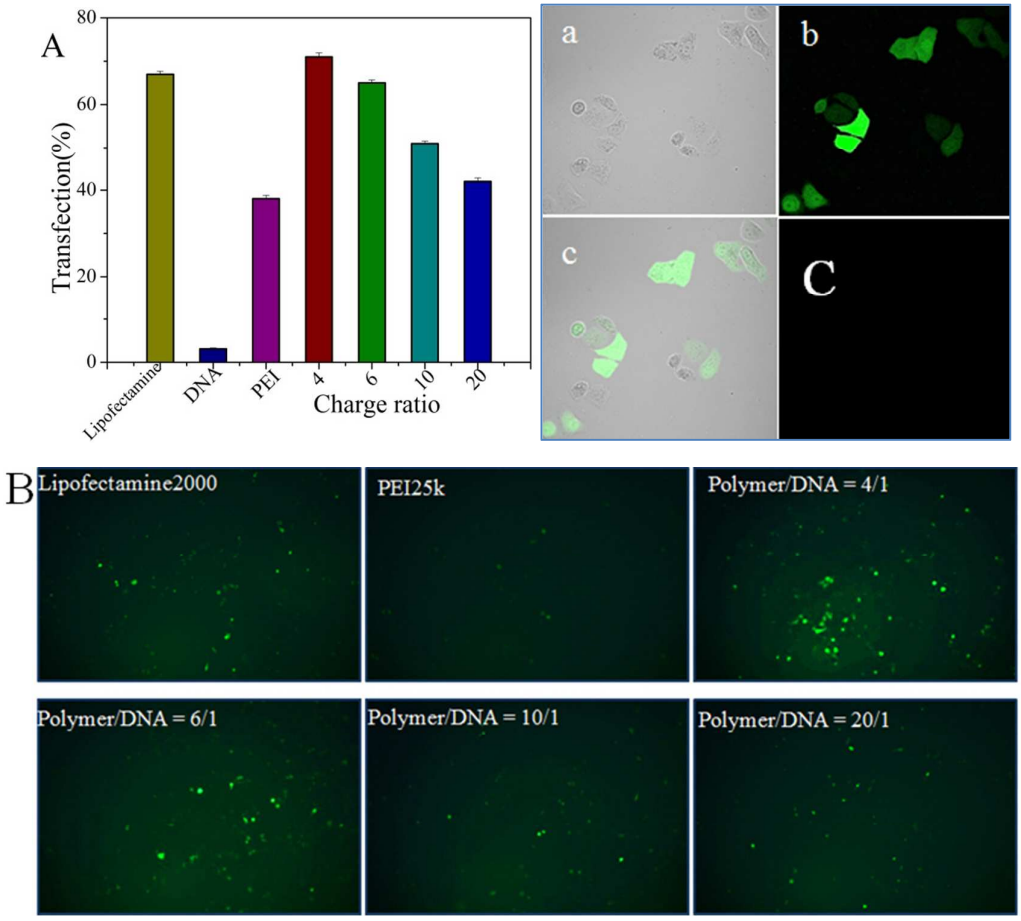

Fig. 6. Percent transfection efficiency(A) and fluorescence microscope images (B) of HepG2 treated with polyplex micelles at different charge ratios and PEI25kD and Lipofectamine2000 complex with pEGFP-C1; Confocal microscopic images of HepG2 cells treated with polyplex micelles at charge ratio of 4/1(C).

4. Conclusion

In summary, a block copolymer with well-defined function was synthesized by RAFT polymerization and used for preparing polyplex micelles as gene vector in vitro. The moiety of PEG-*b*-PAMPImB, PEG segment, imidazolium and amine group of histamine-like segment offered particular contribution to high colloid stability, effective DNA condensation and buffering capacity, resulting in the low toxicity and high gene expression. The polymer architectures based on the relation of structure-function provide a valuable approach for development of safe and highly efficient nonviral gene vectors.

Acknowledgements

This work was supported by the National Natural Science Foundation of China (No.51103035 and 51403055) and Scientific &Technological Project of Henan Province (No.132102310422)

References

1. E. Cederfjall, L. Broom and D. Kirik, ***Mol. Ther.***, 2015, **23**, 896-906.
2. J. H. Kordower, ***Neuropsychopharmacology***, 2015, **40**, 255-256.
3. V. B. Morris and V. Labhasetwar, ***Biomaterials***, 2015, **60**, 151-160.
4. M. A. Cortez, W. T. Godbey, Y. Fang, M. E. Payne, B. J. Cafferty, K. A. Kosakowska and S. M. Grayson, ***J. Am. Chem. Soc***., 2015, **137**, 6541-6549.
5. H. He, Y. Bai, J. Wang, Q. Deng, L. Zhu, F. Meng, Z. Zhong and L. Yin, ***Biomacromolecules***, 2015, **16**, 1390-1400.
6. J. Luo, Y. Luo, J. Sun, Y. Zhou, Y. Zhang and X. Yang, ***Cancer Lett***., 2015, **356**, 347-356.
7. B. Santos-Carballal, L. J. Aaldering, M. Ritzefeld, S. Pereira, N. Sewald, B. M. Moerschbacher, M. Götte and F. M. Goycoolea, ***Scientific Reports***, 2015, **5**, 13567.
8. J. Li, Q. Chen, Z. Zha, H. Li, K. Toh, A. Dirisala, Y. Matsumoto, K. Osada, K. Kataoka and Z. Ge, ***J. Control.Release***, 2015, **209**, 77-87.
9. Q. Wang, J. Li, S. An, Y. Chen, C. Jiang and X. Wang, ***Int. J. Nanomedicine***, 2015, **10**, 4479-4490.
10. L. Feng, X. Yang, X. Shi, X. Tan, R. Peng, J. Wang and Z. Liu, ***Small***, 2013, **9**, 1989-1997.
11. D. Ibraheem, A. Elaissari and H. Fessi, ***Int. J. Pharm.***, 2014, **459**, 70-83.
12. D. W. Pack, A. S. Hoffman, S. Pun and P. S. Stayton, ***Nat. Rev. Drug. Discov.***, 2005, **4**, 581-593.
13. K. Miyata, N. Nishiyama and K. Kataoka, ***Chem. Soc. Rev.***, 2012, **41**, 2562-2574.
14. L. Novo, L. Y. Rizzo, S. K. Golombek, G. R. Dakwar, B. Lou, K. Remaut, E. Mastrobattista,

C. F. van Nostrum, W. Jahnen-Dechent, F. Kiessling, K. Braeckmans, T. Lammers and W. E. Hennink, ***J. Control.Release***, 2014, **195**, 162-175.

15. E. Junquera and E. Aicart, ***Adv. Colloid. Interface. Sci.***, DOI: http://dx.doi.org/10.1016/j.cis.2015.07.003.
16. R. V. Rodik, A.-S. Anthony, V. I. Kalchenko, Y. Mely and A. S. Klymchenko, ***New J. Chem.***, 2015, **39**, 1654-1664.
17. M. Zhang, Q. Xiong, Y. Wang, Z. Zhang, W. Shen, L. Liu, Q. Wang and Q. Zhang, ***Polym. Chem.***, 2014, **5**, 4670-4678.
18. X. Long, Z. Zhang, S. Han, M. Tang, J. Zhou, J. Zhang, Z. Xue, Y. Li, R. Zhang, L. Deng and A. Dong, ***ACS Appl. Mater. Interfaces***, 2015, **7**, 7542-7551.
19. Z. Ge, Q. Chen, K. Osada, X. Liu, T. A. Tockary, S. Uchida, A. Dirisala, T. Ishii, T. Nomoto, K. Toh, Y. Matsumoto, M. Oba, M. R. Kano, K. Itaka and K. Kataoka, ***Biomaterials***, 2014, **35**, 3416-3426.
20. D. G. Abebe, R. Kandil, T. Kraus, M. Elsayed, O. M. Merkel and T. Fujiwara, ***Macromol. Biosci.***, 2015, **15**, 698-711.
21. M. Oba, K. Miyata, K. Osada, R. J. Christie, M. Sanjoh, W. Li, S. Fukushima, T. Ishii, M. R. Kano, N. Nishiyama, H. Koyama and K. Kataoka, ***Biomaterials***, 2011, **32**, 652-663.
22. K. Nagata, K. Itaka, M. Baba, S. Uchida, T. Ishii and K. Kataoka, ***J. Control.Release***, 2014, **183**, 27-34.
23. K. Miyata, R. J. Christie and K. Kataoka, ***React. Funct. Polym.***, 2011, **71**, 227-234.
24. T. Nomoto, Y. Matsumoto, K. Miyata, M. Oba, S. Fukushima, N. Nishiyama, T. Yamasoba and K. Kataoka, ***J. Control.Release***, 2011, **151**, 104-109.
25. J. Deng, N. Gao, Y. Wang, H. Yi, S. Fang, Y. Ma and L. Cai, ***Biomacromolecules***, 2012, **13**, 3795-3804.
26. X. Cai, Y. Li, D. Yue, Q. Yi, S. Li, D. Shi and Z. Gu, ***J. Mater. Chem.B***, 2015, **3**, 1507-1517.
27. B. Shi, H. Zhang, J. Bi and S. Dai, ***Colloids Surf .B Biointerfaces***, 2014, 119, 55-65.
28. J. Gu, X. Chen, H. Xin, X. Fang and X. Sha, ***Int. J. Pharm.***, 2014, **461**, 559-569.
29. W. Xu, P. Ledin, V. Shevchenko, V. Tsukruk, ***ACS Appl. Mater. Interfaces***, 2015, **7**, 12570-12595
30. C. Gonçalves, M. Berchel, M.-P. Gosselin, V. Malard, H. Cheradame, P.-A. Jaffrès, P. Guégan, C. Pichon and P. Midoux, Int. J. Pharm., 2014, **460**, 264-272.
31. K. Manojkumar, K. T. Prabhu Charan, A. Sivaramakrishna, P. C. Jha, V. M. Khedkar, R. Siva, G. Jayaraman and K. Vijayakrishna, ***Biomacromolecules***, 2015, **16**, 894-903.
32. E. B. Anderson and T. E. Long, ***Polymer***, 2010, **51**, 2447-2454.
33. M. H. Allen, M. D. Green, H. K. Getaneh, K. M. Miller and T. E. Long, ***Biomacromolecules***, 2011, **12**, 2243-2250.
34. J. Li, K. Zhang, J. Liang, W. Wu, J. Guo and H. Zhou, ***RSC Adv.***, 2015, **5**, 65690-65696.
35. J. B. Li, S. J. Zhang, J. Liang, W. L. Wu, J. W. Guo and H. Y. Zhou, ***RSC Adv.***, 2015, **5**, 7994-8001.
36. J. Li, J. Liang, W. Wu, S. Zhang, K. Zhang and H. Zhou, ***New J. Chem.***, 2014, 38, 2508-2513.
37. D. Fischer, Y. Li, B. Ahlemeyer, J. Krieglstein and T. Kissel, ***Biomaterials***, 2003, **24**, 1121-1131.
38. CabralH, MatsumotoY, MizunoK, ChenQ, MurakamiM, KimuraM, TeradaY, M. R. Kano, MiyazonoK, UesakaM, NishiyamaN and KataokaK, ***Nat. Nano.***, 2011, **6**, 815-823.

39. A. E. Smith, A. Sizovs, G. Grandinetti, L. Xue and T. M. Reineke, ***Biomacromolecules***, 2011, **12**, 3015-3022.
40. H. Wei, J. A. Pahang and S. H. Pun, ***Biomacromolecules***, 2013, **14**, 275-284.
41. H. Wei, L. R. Volpatti, D. L. Sellers, D. O. Maris, I. W. Andrews, A. S. Hemphill, L. W. Chan, D. S. H. Chu, P. J. Horner and S. H. Pun, ***Angew. Chem. Int. Ed.***, 2013, **52**, 5377-5381.

Graphical abstract

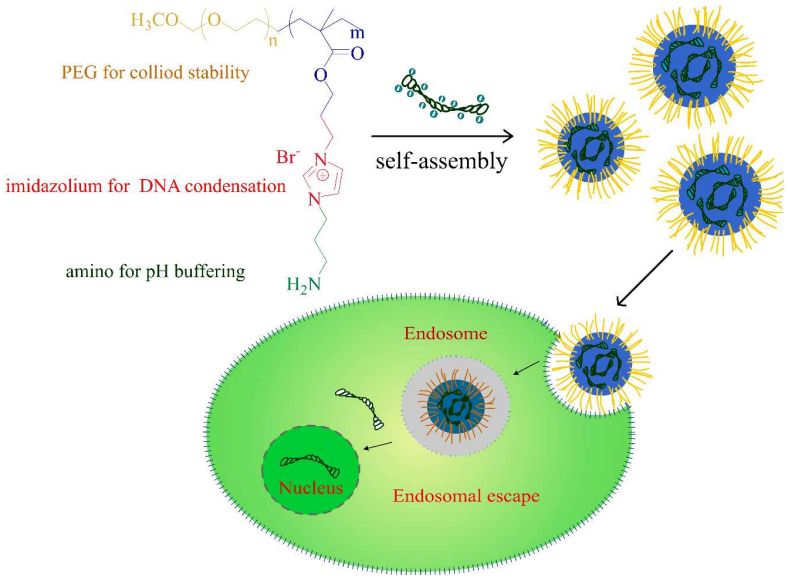

The PEG-*b*-PAMPImB with well-defined function, including high colloid stability, effective DNA condensation and buffering capacity, self-assemble with pDNA for lower toxicity and higher efficient gene transfection.